7. M. A. K. Khalil and R. A. Rasmussen, *Nature* **332**, 242 (1988).
8. _____, in preparation.
9. The Climate Monitoring and Diagnostics Laboratory (CMDL) of the U.S. National Oceanic and Atmospheric Administration (NOAA) operates a global network of sampling sites where air is collected and used to determine the distributions, budgets, and trends of CO_2, CH_4, and CO. Sites are chosen to represent background conditions; that is, to reflect regional-scale processes and not local sources or sinks [T. J. Conway *et al.*, *Tellus Ser. B* **40**, 81 (1988); (*16*)].
10. Two instruments were used for this work, and the instrument response characteristics were described with the use of multiple standards. From July 1988 through December 1990, flask samples were analyzed with an instrument having a linear response over the range of 0 to 1000 ppb of CO (*3*). From January 1991 to June 1993, an instrument with a nonlinear response was used, and a multipoint (seven to nine standards) calibration scheme quantified CO mixing ratios [P. C. Novelli, L. P. Steele, J. W. Elkins, *J. Geophys. Res.* **96**, 13109 (1991)].
11. P. C. Novelli, J. E. Collins Jr., R. C. Myers, G. W. Sachse, H. E. Scheel, *ibid.*, in press. The CMDL calibration procedure is described, and the stabilities of the standards used for both flask sample analysis and calibration of reference gases are reviewed. On the basis of intercomparison of gravimetric standards produced in 1988–1989 and in 1992 and upon intercalibration of working standards, we conclude that the CMDL standard scale has been maintained to a precision of 1% or better. Drift rates in standards were <1% and not significant (2σ).
12. K. W. Thoning, P. P. Tans, W. D. Komhyr, *J. Geophys. Res.* **94**, 8549 (1989). For sites with ≤3 years of data, $np = 2$; for those with >3 years, $np = 3$.
13. P. P. Tans, T. J. Conway, T. Nakazawa, *ibid.* **94**, 5151 (1989).
14. We first used a Delaunay triangulation routine to construct a planar set of points and then created a grid using a linear interpolation.
15. P. Diaconis and B. Efron, *Sci. Am.* **248**, 116 (May 1983).
16. L. P. Steele *et al.*, *Nature* **358**, 313 (1992).
17. Air samples were collected weekly at four high-altitude sites: Niwot Ridge, Colorado (40°N,106°W); Qinghai Province, China (36°N,101°E); Mauna Loa, Hawaii (20°N,156°W); and Tenerife, Canary Islands (28°N,6°W).
18. P. Warneck, *Chemistry of the Natural Atmosphere* (Int. Geophys. Ser. 41, Academic Press, San Diego, CA, 1988), pp. 158–170.
19. R. Prinn *et al.*, *J. Geophys. Res.* **97**, 2445 (1992).
20. P. S. Bakwin, P. P. Tans, P. C. Novelli, *Geophys. Res. Lett.*, in press. The authors model changes in CO over the past 14 years using a simple mass-balance approach. Using CO measurements from Barrow, Alaska; Harvard Forest, Massachusetts; the Atlantic arctic; and Zugspitze, Germany, they concluded CO may have decreased at a rate of 0.9 (±0.5) ppb $year^{-1}$ in the NH solely because of changes in emissions. No significant change was predicted in the SH.
21. J. F. Gleason *et al.*, *Science* **260**, 523 (1993).
22. R. C. Schnell *et al.*, *Nature* **351**, 726 (1991); S. Madronich and C. Granier, *Geophys. Res. Lett.* **19**, 465 (1992), and references therein.
23. R. A. Houghton, *Clim. Change* **19**, 99 (1991); P. M. Fearside, N. Leal Jr., F. M. Fernandes, *J. Geophys. Res.* **98**, 16733 (1993). The NMHC emissions may have decreased because of both economic stagnation and a slowing of deforestation; however, few data are available.
24. G. W. Sachse, R. C. Harriss, J. Fishman, G. F. Hill, D. R. Cahoon, *J. Geophys. Res.* **93**, 1422 (1988); J. Fishman, K. Fakhruzzaman, B. Cros, D. Nganga, *Science* **252**, 1693 (1991); R. A. Delmas, P. Loudjani, A. Podaire, J. C. Menaut, in *Global Biomass Burning*, J. S. Levine, Ed. (MIT Press, Cambridge, MA, 1991), pp. 126–132.
25. We thank N. Zhang for sample analysis, W. Coy and R. Martin for instrument development, and the officers of the M.V. *Wellington Star* (Blue Star Line, London) and personnel at the site locations for the collection of samples. K. Thoning developed many of the smoothing algorithms used here. P. Bakwin provided useful discussions. Funding was provided in part by the Radiatively Important Trace Gas Species component of the NOAA Climate and Global Change Program.

29 November 1993; accepted 2 February 1994

Sound Velocities in Dense Hydrogen and the Interior of Jupiter

Thomas S. Duffy, Willem L. Vos,* Chang-sheng Zha, Russell J. Hemley, Ho-kwang Mao

Sound velocities in fluid and crystalline hydrogen were measured under pressure to 24 gigapascals by Brillouin spectroscopy in the diamond anvil cell. The results provide constraints on the intermolecular interactions of dense hydrogen and are used to construct an intermolecular potential consistent with all available data. Fluid perturbation theory calculations with the potential indicate that sound velocities in hydrogen at conditions of the molecular layer of the Jovian planets are lower than previously believed. Jovian models consistent with the present results remain discrepant with recent free oscillation spectra of the planet by 15 percent. The effect of changing interior temperatures, the metallic phase transition depth, and the fraction of high atomic number material on Jovian oscillation frequencies is also investigated with the Brillouin equation of state. The present data place strong constraints on sound velocities in the Jovian molecular layer and provide an improved basis for interpreting possible Jovian oscillations.

The behavior of hydrogen at high pressure is central to a number of fundamental problems in condensed matter and planetary science (*1*). Measurements of the sound velocity of high-density hydrogen provide critical information on the elastic anisotropy, equation of state (EOS), and other thermodynamic properties of this material. This information is particularly important for the construction of accurate models for the interior structure of the giant planets (*2*). Uncertainty in the EOS of hydrogen is the source of the largest uncertainty in current Jovian models (*3*). Recently, the first successful observations of global free oscillations of Jupiter have been reported (*4*). Such measurements could provide a wealth of new information about the Jovian planets, much as helioseismology has revolutionized understanding of the solar interior. Current interpretations of Jovian oscillation spectra suggest a need for major revisions of interior models (*5*). Free oscillation spectra are sensitive to sound velocities that are directly connected to the EOS in the planet's interior. Thus, measurement of sound velocities in dense hydrogen can provide more direct constraints on the seismic structure of the molecular region of the planet.

We have developed a technique for in situ measurements of the elasticity of hydrogen and similar materials to very high pressures in a diamond anvil cell. We combine acoustic velocities measured by Brillouin scattering with the orientation and number of crystals determined by synchrotron x-ray diffraction. Brillouin scattering uses the frequency shift of laser light scattered by thermally generated sound waves to determine acoustic velocities (*6*). In this study, we have overcome a number of restrictions imposed by the diamond cell on the use of Brillouin scattering at high pressure (*7*). Previously, there have been trade-offs between maximum pressure, number of crystallographic orientations probed, and the ability to separate the acoustic velocity from the refractive index. A complete determination of the elastic properties of anisotropic crystals requires the use of multiple scattering geometries, measurements in many crystallographic directions, and careful characterization of the crystals. The latter is a particular problem for materials that are gases at ambient pressure and whose orientation cannot be controlled when solidified at high pressure in the diamond cell.

The development of single-crystal x-ray diffraction using synchrotron radiation for low atomic number materials has led to significant advances in the understanding of hydrogen and other molecular solids (*8*, *9*). Synchrotron x-ray diffraction measurements on H_2 (*8*, *10*, *11*) tightly constrain the EOS between 5.4 and 42 GPa at room temperature. This EOS is consistent with data obtained by other methods (*12*). In this study, we use a pair potential model

Geophysical Laboratory and Center for High-Pressure Research, Carnegie Institution of Washington, 5251 Broad Branch Road, NW, Washington, DC 20015, USA.

*Present address: van der Waals–Zeeman Laboratorium, Universiteit van Amsterdam, 1018 XE Amsterdam, The Netherlands.

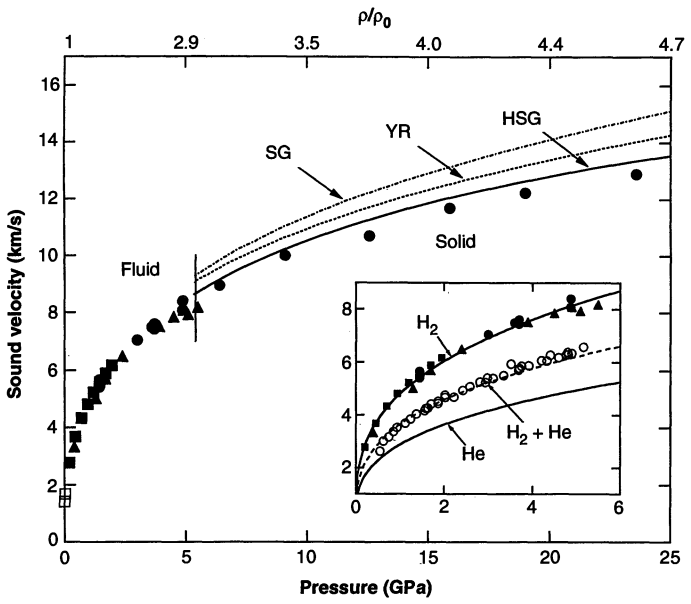

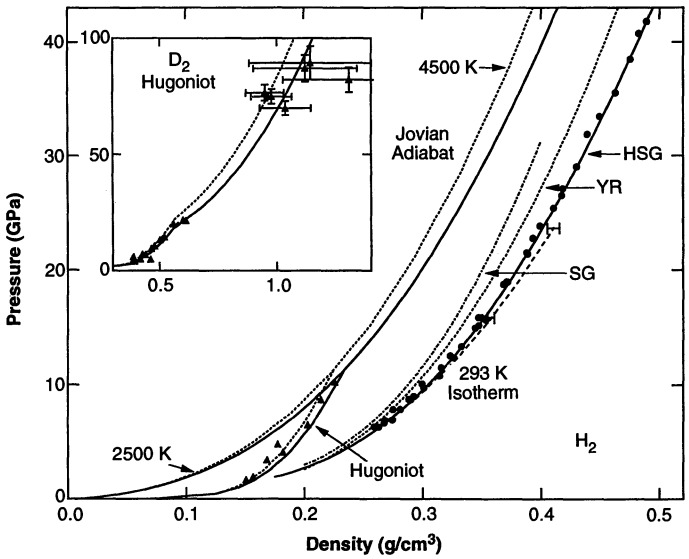

Fig. 1 (left). Hydrodynamic sound velocity in H_2 as a function of pressure. Solid circles, this study; triangles, fluid phase data from (*16*); solid squares, selected data from (*14*); open squares, low-temperature (4 to 13 K) solid data (*35*). Curves show values calculated from the intermolecular potentials [solid line (HSG), this study; short dashed line (YR), (*18*); dash-dot line (SG), (*17*)]. The vertical line is the 293 K melting boundary. The density ratio at top is relative to the ambient pressure, 0 K density of 0.0870 g/cm^3 (*10*). The inset shows data for the fluid H_2-He system. Solid curves are power law fits to data for H_2 [this study (*14, 16*)] and He (*28*). Open circles are calculated from Brillouin frequency shifts for a 50 mol% H_2 mixture of H_2 and He (*7*), and the dashed line is the mixing law calculation (*37*). **Fig. 2 (right).** Equation of state data for hydrogen and deuterium compared with intermolecular potential calculations. Comparisons of the potential models are made for 293 K isotherm data (circles), Hugoniot data (triangles) for H_2 and D_2 (inset), and a Jovian adiabat. Linestyles for the potentials are the same as in Fig. 1. The long dashed line shows the 293 K isotherm derived from Brillouin data. Selected temperatures along the Jovian adiabat are indicated.

that fits both the Brillouin data and existing EOS data to investigate the properties of H_2 at high pressure and temperature, and in particular the *P-T* conditions prevailing within the molecular layer of the Jovian planets.

Brillouin scattering measurements were carried out on both fluid and single-crystal hydrogen compressed at room temperature in a diamond cell (*13*). Figure 1 shows the hydrodynamic or bulk sound velocity, $c = [(\partial P/\partial \rho)_S]^{1/2}$, where P is the pressure and ρ is the density, measured in both this and previous studies. For fluid H_2 (Fig. 1, inset), the bulk sound velocities are directly obtained from Brillouin frequency shifts measured in a 90° scattering orientation. The present results agree well with previous fluid data (*14*). For crystalline H_2, both quasi-compressional and quasi-shear velocities were measured for 15 to 20 separate crystallographic orientations at each of six pressures between 6 and 24 GPa. These data were inverted to obtain the elastic constants, the aggregate bulk and shear moduli, and a self-consistent EOS for H_2 (*15*).

The adiabatic bulk modulus, K_S, and density determine the bulk sound velocity, $c = \sqrt{K_S/\rho}$. Uncertainties in the velocities are approximately ±1% for both fluid and solid phase data. For solid H_2, the bulk sound velocities of this study do not agree with results of previous work (*16*). While the Brillouin measurements themselves are in agreement, the assumption of elastic isotropy and the treatment of quasi-pure modes as pure modes led to an overestimation of the compressibility of solid H_2 by (*16*). The acoustic anisotropy of H_2 is substantial, amounting to 8% for quasi-compressional waves and 18% for quasi-shear waves. This emphasizes the importance of combining Brillouin measurements with a complete crystallographic characterization of the specimen.

The EOS from the Brillouin data is slightly more compressible than that found solely with the x-ray data (*10*), but the EOSs overlap within their mutual uncertainties (Fig. 2). The combined Brillouin–x-ray data set provides a test for intermolecular potentials that are essential for obtaining a thermodynamic description of dense hydrogen at high *P-T* conditions. Figures 1 and 2 show a comparison of sound velocity, static compression, and shock data with the predictions of H_2 potentials (*10, 17, 18*). A large number of H_2 potentials have been proposed; it has been found that the form proposed by Silvera and Goldman (SG) (*17*) can be used as a starting point for describing high-pressure data. The parameters of the SG potential are based on low-pressure (<2 GPa) experimental data that do not adequately include the attractive many-body forces that become important at high pressure. Ross *et al.* (*18*) introduced a modification of this potential (Young-Ross, YR) at short range to fit shock compression data. The shock data (*19*) sample high-temperature fluid states but have larger uncertainties than the static x-ray and sound velocity data. Current models for Jupiter have been constructed with the YR potential (*20, 21*) or an interpolated H_2 EOS (*22*). Hemley *et al.* (*10*) showed that room temperature x-ray diffraction measurements required an additional softening of the YR potential. Here we develop a new form of this potential [Hemley-Silvera-Goldman (HSG)] (*23*) that fits both static compression data (to 42 GPa) and the sound velocity data (Figs. 1 and 2). This potential is also consistent with shock wave data (*24*). With the development of a potential that fits a wide variety of experimental data, including sound velocities, more direct constraints on the properties of the molecular layer of the Jovian planets are obtainable.

A number of models for the interior of Jupiter have been constructed that satisfy observational data for the mass, rotation rate, radius, and gravitational harmonics of the planet (*20–22*). These models consist of a predominantly H_2-He envelope overlying a dense rock and ice core, reaching a central pressure and temperature of ~5000 GPa and ~25,000 K. The envelope is subdivided by the transformation of hydrogen from a low-pressure molecular phase to a high-pressure metallic phase at pressures of ~170 to 500 GPa and temperatures of

10^3 to 10^4 K in current models. An accurate intermolecular potential is needed to reliably extrapolate over the P-T range characterizing the molecular region of the planet.

Major uncertainties in Jovian models include the core size, metallic hydrogen phase transition level, the mass fraction of He (Y), and the EOS of molecular H_2 at densities between 0.1 and 1 g/cm^3. The interior of Jupiter is usually assumed to be fully convective and adiabatic (*2*), but alternative models with compositional gradients have also been proposed (*25*). Assuming the adiabatic model, EOSs were calculated with the YR and HSG potentials and fluid perturbation theory (*26*) for pure H_2 along a Jovian adiabat (T = 165 K at 1 bar) (Fig. 2). At low pressures ($\rho < 0.1$ g/cm^3), there is little difference between the EOSs. At higher pressures, the EOSs diverge such that the HSG EOS is 5 to 9% denser than the YR EOS at P = 25 to 300 GPa. Thus, the experimentally determined potential indicates that molecular H_2 is substantially softer under Jovian conditions than previous models have indicated.

Recently, effort has focused on detecting Jovian global oscillations to obtain better constraints on the interior structure. The successful optical observation of low-degree acoustic oscillations has now been reported in two separate studies by Mosser (*4*). A fundamental parameter derived from the observations is the characteristic frequency or equidistance, ν_0. The equidistance is the inverse of twice the travel time of a ray from the planet's center to the surface

$$\nu_0 = \left[2 \int_0^R dr/c \right]^{-1}$$

where R is the radius of the planet. Although interpretation of currently available spectra is difficult, the observed value of the equidistance is estimated to be 136 ± 10 μHz (*4*) for low-degree modes. In contrast, values of ν_0 computed from existing Jovian models range from 156 to 160 μHz (*5*), a discrepancy of 7 to 27%. If the Jovian observations are correct, a substantial revision of interior models is required. The molecular region (P = 0 to ~2 to 5 Mbar) contributes about 40% to the value of ν_0 for Jupiter. Thus, it is important to consider the extent to which changes in the EOS, temperature, and composition within the molecular region of Jupiter affect the equidistance of Jovian models.

Figure 3 shows sound velocities in H_2 along Jovian adiabats calculated with the HSG and YR potentials. The HSG potential yields sound velocities that are up to 7% lower than the YR potential at high pressure. The Jovian interior model of Chabrier *et al.* (*20*) includes a detailed thermodynamic treatment of dense hydrogen with the YR potential (*27*). The transition to metallic hydrogen (plasma phase) was found to be first-order and to occur at 171 GPa in Jupiter. If the molecular portion of this model is adjusted to reflect the lower sound velocities of Fig. 3, the equidistance for the Jovian interior is reduced by ~1.6%. Although this is in the correct direction to explain the seismic discrepancy, it accounts for only ~10% of the difference between observations and models. Thus, the improved EOS for molecular H_2 can only partially explain the apparently anomalous seismic properties of Jupiter. The magnitude of the change in the H_2 EOS required to fit the seismic data lies well outside of experimental uncertainties in the sound velocity and density data (Fig. 3). The present H_2 EOS at 0 K agrees well with the interpolated 0 K EOS used in the Jupiter models of Zharkov and colleagues (*2*, *22*). This is consistent with the slightly lower equidistance found in those models (*5*). Other features of Jovian models that might need to be modified include the interior temperatures, core size, composition, molecular-metallic phase transition, interior stratification, and the metallic EOS. The required changes are large, however, necessitating approximately a 15% reduction in sound velocity over the planet as a whole.

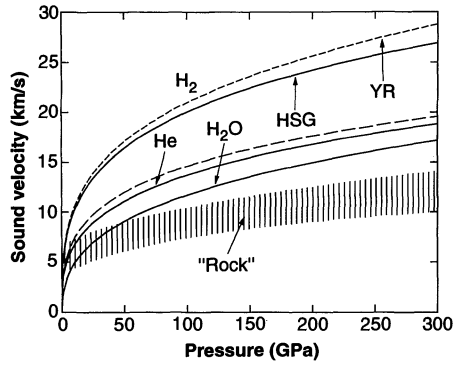

Fig. 3. Sound velocities calculated along a Jovian adiabat with the YR and HSG potentials for H_2. Also shown are sound speeds for some other principal components of Jupiter at the P,T conditions of the pure H_2 Jovian adiabat. For He and H_2O, sound velocities were determined with an exponential-6 potential (*36*), and the range of values for the rock component (hatched region) were estimated from shock compression data. The long dashed curve shows the sound velocities in the molecular region required to satisfy seismic data.

The effect of changes in interior temperatures produced by, for example, a boundary layer near the Jovian surface (*5*) can be assessed by computing adiabats at different starting temperatures. Pure H_2 adiabats at initial temperatures of 65 K and 265 K produce temperatures at the 1- to 2-Mbar level that are found to differ by 5000 to 6000 K, but the sound velocity difference is less than 1% at these pressures. If the sound velocity changes are restricted to the boundary layer itself, the presence of such a boundary is unlikely to produce an appreciable change in the equidistance of a planet that is dominantly adiabatic. Adjusting the metallic phase transition level between 171 and 500 GPa affects the equidistance by 4%, with higher transition pressures corresponding to higher equidistances. If the phase transition occurs continuously over this range, however, the equidistance is reduced relative to its value at 171 GPa by 1 to 2%.

Experimental sound speeds in fluid H_2 and measured Brillouin frequency shifts in He (*28*) and H_2-He (*7*) at high pressure and 293 K can be used to infer the compositional effects on the sound velocities of mixtures relevant to the giant planets. We adopt a model for the H_2-He system in which the refractive index is given by the Lorentz-Lorenz mixing rule (*29*), the density is computed from the additive-volume law [in agreement with (*30*)], and bounds on the bulk modulus are obtained from volume fractions (*31*). This approach reproduces the Brillouin scattering data for a 50 mol percent H_2 mixture of H_2-He (*7*) to 5 GPa (Fig. 1, inset). We therefore adopt this model for preliminary estimates of compositional effects on sound velocities in the Jovian interior. For a homogeneous mixture, approximately doubling the He mass fraction of both the metallic and molecular regions to Y ~ 0.58 is required to reduce the sound velocities in the model of (*20*) by the amount required to satisfy the seismic data. This is far in excess of values from observations of the Jovian atmosphere (Y = 0.18 ± 0.04) (*32*), the expected nebular abundance of He (Y ~ 0.28) (*33*), or current Jovian models [~one-third nonhydrogen by mass, including core (*20*–*22*)]. Whether large increases in the nonhydrogen component can be reconciled with gravity and mean density data needs to be examined in future Jovian models. Assuming nebular abundance of He and attributing the remaining mass excess to the Z (non–hydrogen-helium) component requires enrichment of the Jovian rock plus ice component by a factor of ~23 relative to nebular values, whereas current models have enrichment factors of 3 to 10 (*20*–*22*).

The measurement of sound velocities in dense hydrogen coupled with advances in Jovian seismology presents new opportunities for probing the internal structures of the Jovian planets, which make up more than 99% of the planetary mass of the solar system. Experimental data now constrain the properties of a growing fraction of Jupiter. The large discrepancy with observa-

tional data underscores the need for major revisions of Jovian models beyond features connected to the molecular H_2 EOS or suggests that reanalysis of the free oscillation observations is required.

REFERENCES AND NOTES

1. H. K. Mao and R. J. Hemley, *Am. Sci.* **80**, 234 (1992).
2. V. N. Zharkov, *Interior Structure of the Earth and Planets* (Harwood, New York, 1986).
3. M. Podolak, W. B. Hubbard, J. B. Pollack, in *Protostars and Planets III*, E. H. Levy and J. I. Lunine, Eds. (Univ. of Arizona Press, Tucson, AZ, 1993), p. 1109.
4. B. Mosser, F. X. Schmider, Ph. Delache, D. Gautier, *Astron. Astrophys.* **251**, 356 (1991); B. Mosser *et al.*, *ibid.* **267**, 604 (1993).
5. J. Provost, B. Mosser, G. Berthomieu, *ibid.* **274**, 595 (1993).
6. W. Hayes and R. Loudon, *Scattering of Light by Crystals* (Wiley, New York, 1978).
7. A. Polian, in *Frontiers of High Pressure Research*, H. D. Hochheimer and R. D. Etters, Eds. (Plenum, New York, 1991), p. 181.
8. H. K. Mao *et al.*, *Science* **239**, 1131 (1988).
9. H. K. Mao *et al.*, *Phys. Rev. Lett.* **60**, 2649 (1988); W. L. Vos *et al.*, *Nature* **358**, 46 (1992).
10. R. J. Hemley *et al.*, *Phys. Rev. B* **42**, 6458 (1990).
11. J. Hu, H. K. Mao, J. F. Shu, R. J. Hemley, in *High Pressure Science and Technology–1993*, S. C. Schmidt, J. W. Shaner, G. A. Samara, M. Ross, Eds. (American Institute of Physics, New York, in press).
12. V. V. Matveev, I. V. Medvedeva, V. V. Prut, P. A. Suslov. S. A. Shibaev, *Pis'ma Zh. Eksp. Teor. Fiz* **39**. 219 (1984): V. P. Glazkov *et al.*, *ibid.* **47**, 661 (1988): J. van Straaten and I. F. Silvera, *Phys. Rev. B* **37**. 1989 (1988).
13. Pure hydrogen gas and a grain of ruby were loaded into a 150-μm hole in a rhenium gasket of a large-aperture diamond cell. A number of Brillouin spectra were recorded in the fluid phase between 1.5 and 4.9 GPa. A new sample was then loaded and carefully pressurized above the room-temperature freezing point (5.4 GPa) to form a single crystal. Pressures were measured from the frequency shift of the R_1 fluorescence line of ruby [H. K. Mao, J. Xu, P. M. Bell, *J. Geophys. Res.* **91**, 4673 (1986)]. The number of crystals and their orientation were determined at each pressure by synchrotron x-ray diffraction at beamline X17C of the National Synchrotron Light Source, Brookhaven National Laboratory. Brillouin scattering measurements were carried out with a newly constructed spectrometer utilizing a six-pass tandem Fabry-Perot interferometer [R. Mock, B. Hillebrands, J. R. Sandercock, *J. Phys. E.* **20**, 656 (1987)]. A single-frequency Ar^+ laser served as the excitation source. The system was designed to allow for a number of different scattering geometries. Most of the data were collected with use of a 90° geometry. Other data were collected in a backscattering geometry, which is sensitive to the product of refractive index and velocity. Further experimental details are presented elsewhere (*34*).
14. R. L. Mills, D. H. Liebenberg, J. C. Bronson, L. C. Schmidt, *J. Chem. Phys.* **66**, 3076 (1977); E. M. Brody, H. Shimizu, H. K. Mao, P. M. Bell, W. A. Bassett, *J. Appl. Phys.* **52**, 3583 (1981).
15. The Brillouin and crystallographic data were inverted with use of Christoffel's equation to obtain the five independent elastic constants of hexagonal H_2. The adiabatic bulk and shear moduli were obtained by orientationally averaging the individual constants. The isothermal bulk modulus was computed from the adiabatic value by making a small thermodynamic correction. The EOS was calculated by integrating over the isothermal bulk modulus (*34*).
16. H. Shimizu, E. M. Brody, H. K. Mao, P. M. Bell, *Phys. Rev. Lett.* **47**, 128 (1981).
17. I. F. Silvera and V. V. Goldman, *J. Chem. Phys.* **69**, 4209 (1978).
18. M. Ross, F. H. Ree, D. A. Young, *ibid.* **79**, 1487 (1983).
19. M. van Thiel *et al.*, *Phys. Earth Planet. Int.* **9**, 57 (1974); R. D. Dick and G. I. Kerley, *J. Chem. Phys.* **73**, 5264 (1980); W. J. Nellis, A. C. Mitchell, M. van Thiel, G. J. Devine, R. J. Trainor, *ibid.* **79**, 1480 (1983).
20. G. Chabrier, D. Saumon, W. B. Hubbard, J. I. Lunine, *Astrophys. J.* **391**, 817 (1992).
21. W. B. Hubbard and M. S. Marley, *Icarus* **78**, 102 (1989).
22. T. V. Gudkova, V. N. Zharkov, V. V. Leont'ev, *Solar Sys. Res.* **22**, 159 (1989); V. N. Zharkov and T. V. Gudkova, *Ann. Geophysicae* **9**, 357 (1991).
23. The potential, ϕ, describes effective isotropic pair-wise interactions and includes many-body terms implicitly. It is based on the form (*17*)

$$\phi(r) = \exp(\alpha - \beta r - \gamma r^2) - \left(\frac{C_6}{r^6} + \frac{C_8}{r^8} + \frac{C_{10}}{r^{10}}\right) f(r) + \frac{C_9}{r^9} f(r)$$

where $f(r)$ is a damping function given by

$$f(r) = \exp\left[-\left(\frac{1.28 r_m}{r} - 1\right)^2\right] \quad r < 1.28 r_m$$
$$= 1.0 \quad r > 1.28 r_m$$

where r is the intermolecular spacing, r_m is the position of the potential well minimum, and the other parameters are constants. The potential also includes a short-range term of the form

$$V_{SR} = a_1(r - r_c)^3 + a_2(r - r_c)^6 \quad r \le r_c$$
$$= 0 \quad r > r_c$$

The parameters of the short-range term are as follows: $a_1 = 4.213 \times 10^{-4}$ hartree/bohr^3, $a_2 = -8.045 \times 10^{-5}$ hartree/bohr^6, with $r_c = 5.2912$ bohr. Values of the other parameters are given in (*17*). We emphasize that this is an effective potential for both the solid and fluid phases. Alternatively, one could develop effective potentials appropriate for the two phases (state-dependent potentials). These could differ as a result of possible differences in intermolecular interactions in the two phases, in particular when comparing the room-temperature solid and the shocked fluid (that is, owing to differences in rotational and vibrational excitations). Despite this, we find that the potential provides a very good fit to all high-pressure data (Figs. 1 and 2). Additional constraints on the potential could be obtained from temperature measurements along the Hugoniot (W. J. Nellis, personal communication).
24. Hugoniot curves were calculated by the method described in (*18*), except that dissociation was not included in the calculation.
25. D. J. Stevenson, *Icarus* **62**, 4 (1985).
26. M. Ross, *J. Chem. Phys.* **71**, 1567 (1979). No dissociation was allowed in the adiabat calculations. See (*18*) and (*27*) for additional details and discussion.
27. D. Saumon and G. Chabrier, *Phys. Rev. A* **44**, 5122 (1991); *ibid.* **46**, 2084 (1992).
28. R. Le Toullec, P. Loubeyre, J.-P. Pinceaux, *Phys. Rev. B* **40**, 2368 (1989); A. Polian and M. Grimsditch, *Europhys. Lett.* **2**, 849 (1986).
29. W. Heller, *J. Phys. Chem.* **69**, 1123 (1965); H. Craig, *Geochim. Cosmochim. Acta* **56**, 3001 (1992).
30. L. C. van den Bergh and J. A. Schouten, *J. Chem. Phys.* **89**, 2336 (1988).
31. J. P. Watt, G. F. Davies, R. J. O'Connell, *Rev. Geophys. Space Phys.* **14**, 541 (1976); H. T. Hammel, *Phys. Chem. Liq.* **14**, 171 (1985).
32. D. Gautier and T. Owen, in *Origin and Evolution of Planetary Atmospheres*, S. K. Atreya, J. B. Pollack, M. S. Matthews, Eds. (Univ. of Arizona Press, Tucson, AZ, 1989), p. 487.
33. B. Conrath, D. Gautier, R. Hanel, G. Lindal, A. Marten, *J. Geophys. Res.* **92**, 15003 (1987); E. Anders and N. Grevesse, *Geochim. Cosmochim. Acta* **53**, 197 (1989).
34. C. S. Zha, T. S. Duffy, R. J. Hemley, H. K. Mao, *Phys. Rev. B* **48**, 9246 (1993).
35. R. Wanner and H. Meyer, *J. Low Temp. Phys.* **11**, 715 (1973); P. J. Thomas, S. C. Rand, B. P. Stoicheff, *Can. J. Phys.* **56**, 1494 (1978).
36. F. H. Ree, in *Simple Molecular Systems at Very High Density*, A. Polian, P. Loubeyre, N. Boccara, Eds. (Plenum, New York, 1989), p. 153.
37. These results are consistent with another recent analysis of the data in (*7*) (P. Loubeyre, personal communication).

38. We thank J. F. Shu and J. Z. Hu for assistance in the x-ray diffraction measurements and M. S. Marley, D. Saumon, and P. Loubeyre for useful correspondence. We are also grateful to M. Ross, W. J. Nellis, D. Saumon, and A. Boss for comments and discussion. Supported by NSF and NASA.

29 October 1993; accepted 3 February 1994

Short-Lived Chemical Heterogeneities in the Archean Mantle with Implications for Mantle Convection

Janne Blichert-Toft and Francis Albarède

The neodymium isotope and samarium-neodymium systematics of 2.7-billion-year-old mantle-derived magmas indicate that the lifetime of chemical heterogeneities was much shorter in the Archean mantle than in the modern mantle. Isotopic evidence is compatible with a Rayleigh number 100 times larger and convection 10 times faster in the Late Archean compared with the present-day mantle. Modern plate tectonics thus may be an improbable analog for the Archean. Chemical heterogeneities in the mantle may originate upon magma migration and mineralogical phase changes rather than by recycling of oceanic and continental crust.

The extent of mantle heterogeneity in Archean time is considerably more elusive than that in the modern mantle. Preservation of pre-Phanerozoic mid-ocean ridge basalts is uncertain, and other mantle-derived rocks in the Archean, such as komatiites and continental basalts, may have been contaminated by crustal material (*1*). In addition, the resolution of isotopic data is, from the nature of radiogenic decay, smaller in the Archean than at present.

The development of isotopic heteroge-